Journal Pre-proof

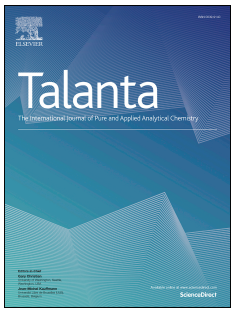

Ultrasensitive electrochemical assay for microRNA-21 based on CRISPR/Cas13a-assisted catalytic hairpin assembly

Ying Cui, Shanji Fan, Ze Yuan, Minghui Song, Jiawen Hu, Dong Qian, Deshuai Zhen, Junhua Li, Baode Zhu

PII: S0039-9140(20)31169-3

DOI: https://doi.org/10.1016/j.talanta.2020.121878

Reference: TAL 121878

To appear in: *Talanta*

Received Date: 3 September 2020

Revised Date: 2 November 2020

Accepted Date: 5 November 2020

Please cite this article as: Y. Cui, S. Fan, Z. Yuan, M. Song, J. Hu, D. Qian, D. Zhen, J. Li, B. Zhu, Ultrasensitive electrochemical assay for microRNA-21 based on CRISPR/Cas13a-assisted catalytic hairpin assembly, *Talanta*, https://doi.org/10.1016/j.talanta.2020.121878.

Credit Author Statement

Conceptualization, Y.Cui. and S.Fan.; Methodology, Y.Cui. and S.Fan. and B. Zhu.; Investigation, S.Fan., Z.Yuan., M.Song, and D.Qian.; Writing – Original Draft, Y.Cui., S.Fan., D.Zhen., J.Hu., and S.Fan.; Writing – Review & Editing, J.Hu. and B. Zhu.; Funding Acquisition, J. Li. and B. Zhu.; Supervision, B. Zhu.

Graphical Abstract

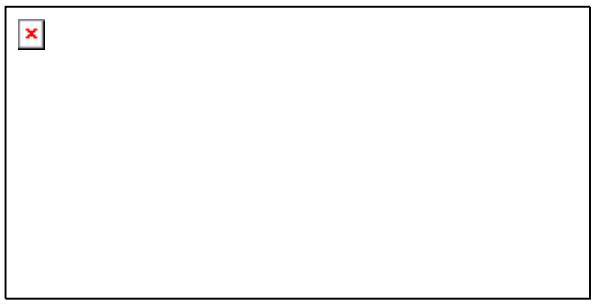

An ultrasensitive electrochemical biosensing platform has been proposed for miRNA-21 assay based on CRISPR/Cas13a-assisted catalytic hairpin assembly.

Ultrasensitive electrochemical assay for microRNA-21 based on CRISPR/Cas13a-assisted catalytic hairpin assembly

Ying Cui,[1,2,a] Shanji Fan,[5,a] Ze Yuan,[1] Minghui Song,[1] Jiawen Hu,[1] Dong Qian,[4] Deshuai Zhen,[1]* Junhua Li,[2]* Baode Zhu[3]*

[1]Hunan Key Laboratory of Two-Dimensional Materials, Advanced Catalytic Engineering Research Center of the Ministry of Education, and College of Chemistry and Chemical Engineering, Hunan University, Changsha 410082, China

[2]College of Chemistry and Materials Science, Hengyang Normal University, Hengyang 421001, China

[3]College of Chemistry Biology & and Environmental Engineering, Xiangnan University, Chenzhou 423043, China

[4]Hunan Provincial Key Laboratory of Chemical Power Resources, College of Chemistry and Chemical Engineering, Central South University, Changsha 410083, PR China

[5]Department of Thyroid Breast Surgery, The First Affiliated Hospital of University of South China, Hengyang 421001, China

[a]These authors contributed equally to this work.

*To whom correspondence should be addressed:

E-mail: deshuaizhen@hnu.edu.cn; junhua325@126.com; baodezhu@xnu.edu.cn

Abstract: MicroRNAs (miRNAs) are related to many biological processes and regarded as biomarkers of disease. Rapid, sensitive, and specific methods for miRNA assay are very important for early disease diagnostic and therapy. In the present work, an ultrasensitive electrochemical biosensing platform has been developed for miRNA-21 assay by combining CRISPR-Cas13a system and catalytic hairpin assembly (CHA). In the presence of miRNA-21, it would hybridize with the spacer region of Cas13a/crRNA duplex to activate the cleavage activity of CRISPR-Cas13a system, leading to the release of initiator of CHA to generate amplified electrochemical signals. Base on the CRISPR-Cas13a-mediated cascade signal amplification strategy, the developed electrochemical biosensing platform exhibited high sensitivity with a low detection limit of 2.6 fM (S/N = 3), indicating that the platform has great potential for application in early clinical diagnostic.

Keywords: Electrochemical biosensor, CRISPR-Cas13a system, catalytic hairpin assembly, cascade signal amplification, miRNA-21

1. Introduction

MicroRNA (miRNA) is a kind of non-coding small RNA molecule (18~25 nucleotides in length), which has crucial regulatory influences in the various biological processes of organisms. Recent researches have confirmed that miRNAs participate in the tissue differentiation, cell proliferation, and other disease state processes [1,2]. Abnormal expression of miRNAs may be related to the occurrence of cancer disease, such as lung cancer, breast cancer, and gastric cancer. Furthermore, even low-level changes on miRNA can dramatically affect the genes expression [3]. Hence, the accurate miRNA determination is important to biomedical research, early cancer diagnostic, prognosis and prediction. However, traditional methods for miRNA detection, such as oligonucleotide microarrays, northern blotting, and quantitative RT-PCR, have some shortcomings in practical applications including time-consuming operation and require extremely precise equipments [4–9]. Therefore, it is still desirable and meaningful to develop biosensing platforms for high-sensitivity assay of miRNA with low requirements for equipments and operational skills.

Recently, the electrochemical biosensors are becoming a powerful detection tool and have aroused great interest due to their good selectivity, sensitivity, and cheap instruments [10, 11]. In view of these advantages, Zhu *et al.* proposed a label-free electrochemical biosensor for microRNA-21 assay using thionine and gold nanoparticles Co-functionalized MoS_2 nanosheet [12]. To further improve the analytical performance, various signal amplification techniques have been adopted in the electrochemical biosensors for miRNA determination, such as rolling circle amplification (RCA) [13], strand displacement amplification (SDA) [14], exponential amplification reaction (EXPAR) [15], hybridization chain reaction (HCR) [16], and catalytic hairpin assembly (CHA) [17]. Among these nucleic acids-mediated signal amplification technologies, CHA is often used for the build of sensing platform due to its excellent signal amplification efficiency. As an enzyme-free nucleic acids-mediated signal amplification technique, CHA can provide transducing and amplifying signals for nucleic acid targets. During the CHA reaction, only in the presence of a trigger,

two hairpins can hybridize with each other to form double-stranded structures, leading to the recycle of the trigger and hundred-fold catalytic amplification [18-20]. Inspired by the advantages of CHA, we are interested in expanding the application scope of the clustered regularly interspaced short palindromic repeat (CRISPR)-associated (Cas) system to miRNA detection using CHA as an amplifier.

As an RNA-guided adaptive immune system, the CRISPR-Cas system was first found in the bacteria and archaeal [21,22]. In the CRISPR family, the CRISPR-Cas12/14 systems have the nonspecific-cleavage activity (*trans*-cleavage) on DNA substrates after specific recognition of target DNA, while the CRISPR-Cas13 system has the *trans*-cleavage activity on RNA substrates after specific recognition of target RNA, thus, the CRISPR-Cas systems are expected to provide rapid, portable, and sensitive diagnostic tools [23−27]. In the past few years, various CRISPR-Cas-assisted analytical platforms for infectious and noninfectious diseases have promoted the development of next-generation diagnostic technology [28−33], which can be applied to the determination of nucleic acids *in vitro* and *in vivo* [34,35]. As we all know, Cas13a protein can combine with crRNA to form a crRNA-guided RNA-activated Cas13a/crRNA ribozyme, which can cleave ~10^4 nonspecific RNAs at physiological temperature in the presence of target RNA, resulting in a four orders of magnitude signal amplification to enhance the detectability [36−40]. Therefore, it is expected that the analytical performance will be further improved by adopting the cascade signal amplification strategy combined CRISPR-Cas13a system and CHA. However, as far as we know, no related studies have been reported through adopting this cascade signal amplification strategy for electrochemical assay of miRNA.

Herein, an ultrasensitive electrochemical biosensing platform has been built for miRNA-21 determination based on the combination of CRISPR-Cas13a system and CHA reaction. In this assay, as shown in Scheme 1, the hairpin DNA 1 (H1) probes were first assembled on the surface of gold (Au) electrode through Au-S bond, and then blocked with 6-mercapto-1-hexanol (MCH) to form the biosensing electrode. In the presence of target miRNA (miRNA-21 was used as the model), the target miRNA would hybridize with the spacer region of the Cas13a/crRNA duplex to activate the

trans-cleavage activity of CRISPR-Cas13a system, leading to the cleavage of plentiful hairpin DNA 0 (H0, containing RNA sequence used as the *trans*-cleavage site) to release the secondary target DNA fragments (ST). Subsequently, the ST strands were used as the initiator of CHA reaction, that is, the ST strands would first hybridize with H1 on the surface of Au electrode, and then the opened H1 hybridized with the methylene blue (MB)-labeled hairpin DNA 2 (H2) to release ST strands for the next cycle. As a consequence, the MB tags closed to the Au electrode surface to generate amplified electrochemical signals. By employing the CRISPR-Cas13a-mediated cascade signal amplification strategy, the electrochemical biosensor displayed a good linear relationship from 10 fM to 1 nM with a detection limit of 2.6 fM (S/N = 3). Therefore, the biosensing platform is a promising analytical method for bioanalysis or even clinical diagnostic.

Scheme 1. Schematic diagram of electrochemical assay for miRNA based on CRISPR-Cas13a system and CHA reaction.

2. Experiment section

2.1. Reagents and apparatus

All oligonucleotides (Table S1) and diethyl pyrocarbonate (DEPC) water used in the study were obtained from Sangon Biotech (Shanghai, China). Cas13a protein was

purchased from Bio-lifesci (Guangzhou, China). Tris(2-carboxyethyl)phosphine (TCEP), N,N,N',N'-Tetramethylethylenediamine (TEMED), SYBR Green I, NaCl, KCl, $MgCl_2$, 6-mercapto-hexanol (MCH), human serum, tris base, and ethanol were supplied by Sigma-Aldrich Inc. (Shanghai, China). 40% acrylamide and bis acrylamide solution (19:1), ammonium persulphate (APS), 6× Loading buffer, and 10× TBE buffer were purchased from Sangon Biotech (Shanghai, China). Gel Imaging System was used for photographing (Bio-Rad, California, USA). An electrochemical workstation (CHI660E, Shanghai, China) was adopted in the study. A three-electrode system was used including a platinum wire as the counter electrode, a planar Au electrode as the working electrode, and a saturated calomel reference electrode (SCE).

2.2. Preparation of the MCH/H1/Au electrode

The Au electrode was first carefully burnished for 3 min by using 0.5 and 0.05 μm alumina oxide slurries, respectively, and then successively sonicated the electrodes in ultrapure water and ethanol for 3 min. Next, the resulted electrodes were immersed for 10 min in a fresh-prepared piranha solution (H_2SO_4:H_2O_2 = 3:1, *v*/*v*) and completely rinsed by using water. Subsequently, the above electrodes were immersed in 0.5 M H_2SO_4 solution and scanned from −0.3 to 1.5 V until a stable cyclic voltammogram (CV) was obtained. After that, the electrodes were rinsed by water and dried at room temperature. Prior to the modification of H1 onto the Au electrode surface, H1 strands were immersed in 20 mM TCEP solution for 0.5 h in the dark. After that, 10 μL of 1 μM H1 were dropped on the Au electrode surface and incubated for 1 h at 37 °C to obtain H1/Au electrode. Finally, the resulted electrodes were immersed in 2 mM MCH solution for 0.5 h to obtain the MCH/H1/Au electrode.

2.3. Native polyacrylamide gel electrophoresis (PAGE) analysis

First, 10% native PAGE was prepared by using 40% acrylamide and bis acrylamide solution (19:1) in 1× TBE buffer containing 0.04% APS and 0.1% TEMED. After the preparation of PAGE, added the mixture of 4 μL samples, 1 μL 6× Loading buffer, and 1 μL SYBR Green I into the gel wells. Then the gel was run at 130 V for 45 min, and

then photographed by a Gel Imaging System.

2.4. Electrochemical analysis of miRNA-21

20 μL of CRISPR-Cas reaction was carried out in the reaction buffer (10 mM Tris-HCl, 50 mM KCl, 1.5 mM $MgCl_2$) including 1 μL of 0.4 μM Cas13a protein, 1 μL of 0.4 μM crRNA, 4 μL of 5 μM H0, and 2 μL various concentrations of miRNA-21, and kept for 1 h at 37 °C. After that, the result solution and 5 μL of 2 μM H2 were dropped on the MCH/H1/Au electrode surface, and kept at 37°C for 1 h. Finally, after washing step, the differential pulse voltammetry (DPV) was performed to measure the biosensing electrodes in 10 mM dioxygen-removed PBS buffer (5 mM $MgCl_2$, 50 mM NaCl, pH 7.4) (The hairpin structures of H0, H1, and H2 are displayed in Fig. S1).

3. Results and discussion

3.1. Characterization of electrode modification

To confirm the modification process, the electrochemical impedance spectroscopy (EIS) was employed to characterize the stepwise modification on the Au electrode surface by using the redox couple of 5 mM $[Fe(CN)_6]^{3-/4-}$ (1:1) in 0.1 M KCl. In a typical EIS, the high-frequency semicircle section corresponds to the charge-transfer limited process, and the augment of the semicircle diameter indicates the increase of the electron-transfer resistance (R_{et}) [41,42]. As shown in Fig. 1A, there was a very small semicircular domain for the bare Au electrode (curve a). After the fabrication of H1 on the Au electrode surface, an obvious change was observed (curve b) because of the repulsive interaction between $[Fe(CN)_6]^{3-/4-}$ and negative charges on H1 strands. When the above electrode was blocked with MCH, the R_{et} value further increased (curve c). After the addition of CRISPR-Cas13a reaction solution and H2 strands, the R_{et} value increased significantly due to the formation of H1-H2 duplex (curve d). Furthermore, the cyclic voltammetry (CV) was also performed to confirm the stepwise modification process at a scan rate of 0.1 V/s. As displayed in Fig. 1B, a pair of well-defined peaks could be observed for the bare Au electrode due to its

outstanding electric conduction (curve a). With the assembly of H1 and MCH, and the formation of H1-H2 duplex, the peak current decreased gradually (curves b to d). These results in Fig. 1B are consistent with that exhibited in the EIS measurements (Fig. 1A), indicating the successful assembly process of the developed biosensing platform.

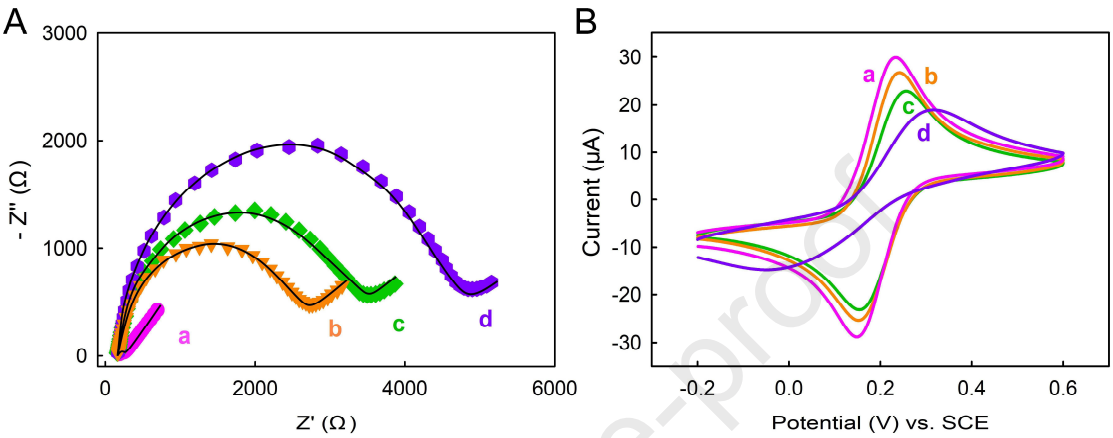

Fig. 1. (A) EIS and (B) CV for stepwise modification on the Au electrode surface (a) bare Au electrode, (b) H1/Au electrode, (c) MCH/H1/Au electrode, (d) H2/MCH/H1/Au electrode. The black solid lines in EIS measurements are fitted Nyquist plots.

3.2. Feasibility of the biosensing platform for miRNA-21 assay

To confirm the feasibility, DPV technique was adopted. As displayed in Fig. 2A, compared to the reaction system without miRNA-21 (curve a), the peak current increased dramatically in the presence of 10 pM miRNA-21 (curve b), demonstrating that miRNA-21 could indeed cause the increase of the electrochemical signal. Subsequently, 10% PAGE analysis was employed to further validate the feasibility of the detection system. As shown in Fig. 2B, the bands of H0, H1, and H2 could be observed in lanes 1-3, respectively. Compared to lane 4 without miRNA-21, the bands of H0, H1, and H2 almost disappeared and the new bands of cleaved H0, ST strands, and H1-H2 duplex in lane 5, which could be because in the presence of miRNA-21, the activated Cas13a/crRNA system cleaved the H0 to generate ST strand and cleaved H0 fragment, and the ST strand initiated the subsequent CHA reaction to produce H1-H2 duplex. In addition, since the Cas13a/crRNA duplex was blocked in the PAGE

wells, it cannot be observed on PAGE. Hence, the PAGE results were highly consistent with the results of the electrochemical signal, verifying the satisfactory feasibility for miRNA-21 assay.

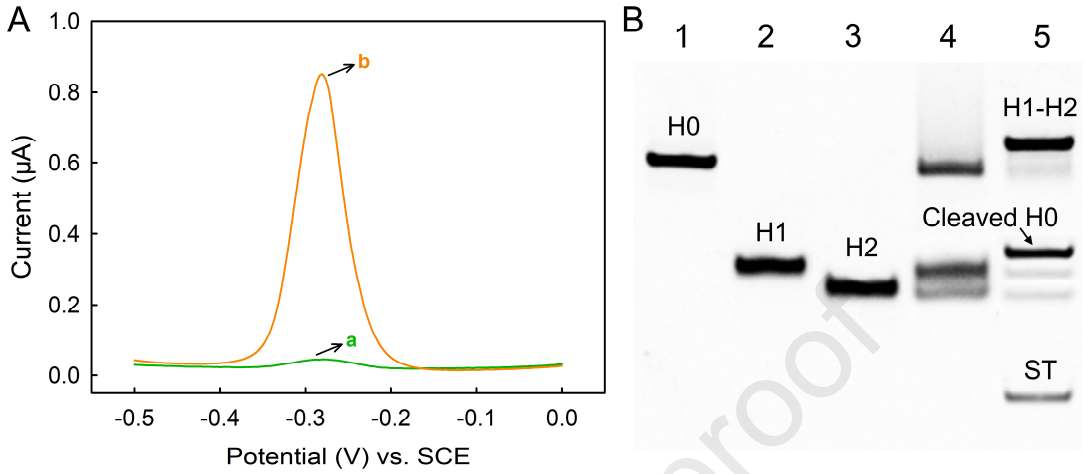

Fig. 2. Feasibility of the electrochemical biosensing platform. (A) DPV curves of (a) the reaction system without miRNA-21, (b) the reaction system with 10 pM miRNA-21. (B) 10% PAGE analysis of the biosensing system. Lane 1: 5 μM H0; lane 2: 5 μM H1; lane 3: 5 μM H2; lane 4: 5 μM H0, 2 μM H1, 2 μM H2, 0.4 μM Cas13a protein, and 0.4 μM crRNA; lane 5: 5 μM H0, 2 μM H1, 2 μM H2, 0.4 μM Cas13a protein, 0.4 μM crRNA, and 10 pM miRNA-21.

3.3. Optimization of the biosensing platform

Prior to obtaining the best analytical performance for miRNA-21 determination, some important experimental parameters should be optimized. First, the spacer length of crRNA was investigated from 14 to 22 nt in the presence of 10 pM miRNA-21, the results demonstrated that the spacer length of 20 nt is sufficient for the generation of *trans*-cleavage activity (Fig. 3A and B). Subsequently, as shown in Fig. 3C, the complementary base number (the stem region in the dashed box) of H0 is a key factor affecting the signal-to-background ratio of the biosensing system. In the absence of miRNA-21, with the increase of complementary base number, the peak current decreased gradually because of the decreasing background of the detection system, which is attributed to the fact that the hairpin structures gradually became more stable with the increase of complementary base number. However, there was no great change in the peak current at first with 10 pM miRNA-21, and then it gradually decreased.

This result indicated that although the *trans*-cleavage activity of the CRISPR-Cas13a system was activated by miRNA-21, the stem region of H0 was very stable due to the excessive complementary base numbers, which made it difficult for the release of ST strands to trigger the following CHA reaction, so there was no distinct increase in the peak current. Therefore, the 12-complementary base was selected in this study because of the maximum signal-to-background ratio. The cleavage time is another important parameter because it is related to the yield of ST strands. As exhibited in Fig. 3D, with the increase of cleavage time, the peak current enhanced and then reached a plateau at the time of 1 h, so 1 h was chose as the optimized cleavage time. Subsequently, the cleavage temperature was also evaluated (Fig. 3E), the peak current enhanced with the increased temperature and achieved a maximum value at 37 °C. When the temperature further increased, the peak current decreased because the high temperature could influence the activity of Cas13a protein. Thus, 37 °C was used in the CRISPR-Cas13a reaction system. Finally, we assessed the effect of CHA reaction time (Fig. 3F), the peak current achieved a plateau at 1.5 h, so 1.5 h was adopted as the optimized CHA reaction time.

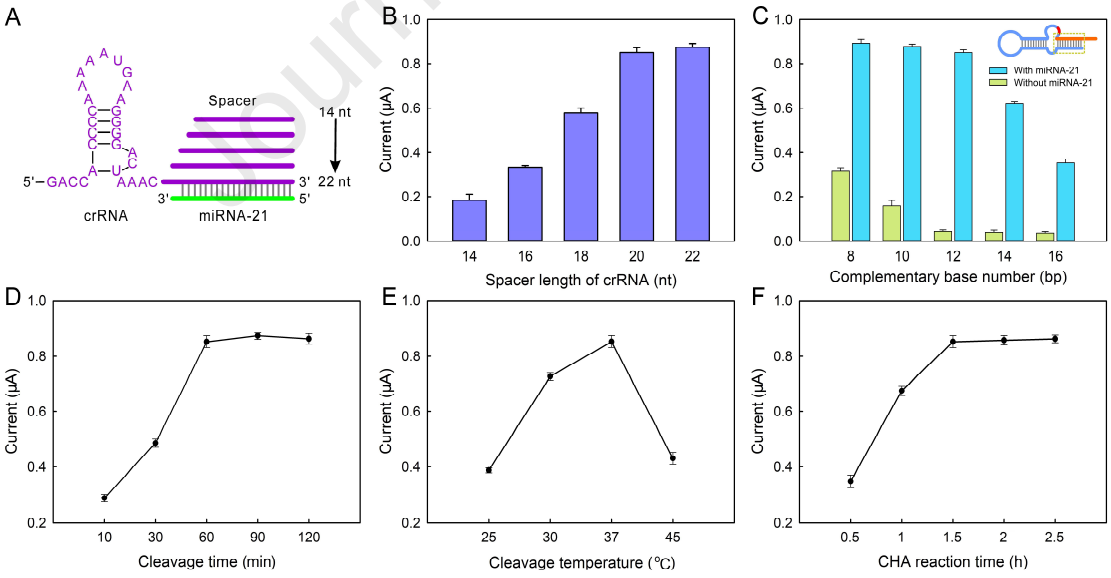

Fig. 3. Optimization of experimental parameter with 10 pM miRNA-21. (A) Schematic illustration of spacer length with 14−22 nt, (B) Evaluation of the influence of the spacer length, (C) Complementary base number of the stem region of H0, (D) Cleavage time, (E) Cleavage temperature, (F) CHA reaction time. Error bars are

standard deviations of three parallel experiments.

3.4. Quantification of target miRNA-21

Under optimized experimental conditions, we investigated the sensitivity of the proposed biosensing platform with varied miRNA-21 concentrations from 0 to 10 nM. The peak current of MB increased with the increase of miRNA-21 concentrations (Fig. 4A). Moreover, the peak currents maintained a good linear relationship with the logarithmic concentrations of miRNA-21 from 10 fM to 1 nM, and the linear equation was I (μA) = 0.2543 lg $C_{\text{target (pM)}}$ + 0.5970 (R^2 = 0.9966) with a detection limit of 2.6 fM (S/N = 3) (Fig. 4B), indicating much better analysis capability than most of the previously reported analytical methods (Table S2).

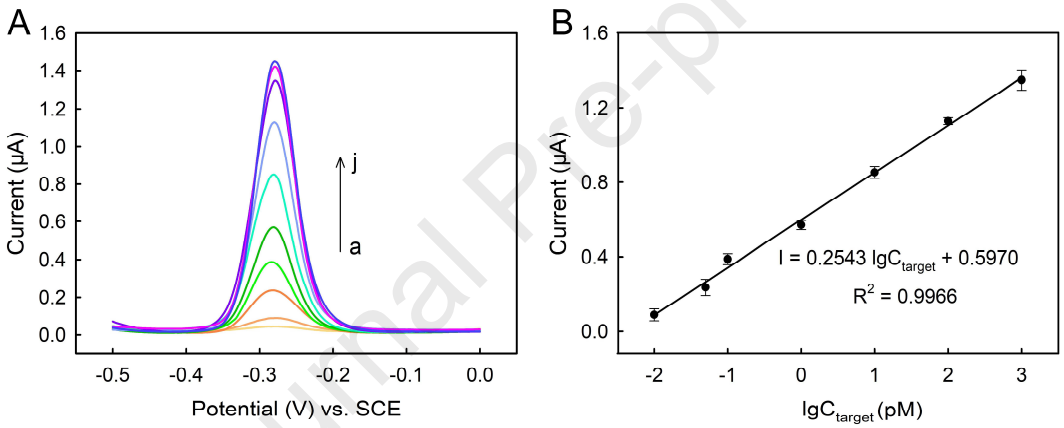

Fig. 4. (A) DPV curves of the biosensing platform responded to various concentrations of miRNA-21. (a–j) 0 fM, 10 fM, 50 fM, 100 fM, 1 pM, 10 pM, 100 pM, 1 nM, 5 nM, and 10 nM. (B) Linear plot of peak currents *vs.* logarithm of miRNA-21 concentrations from 10 fM to 1 nM. Error bars are standard deviations of three parallel experiments.

3.5. Stability, reproducibility, and specificity of the developed platform

First, we evaluated the stability of the developed platform through storing the biosensing electrodes at 4 °C for 2 weeks, as shown in Fig. S2, three parallel tests verified that the peak currents could maintain about 98.3% of their original values for 10 pM miRNA-21 assays. Next, we investigated the reproducibility via testing five biosensing electrodes in the presence 10 pM miRNA-21, and replicate measurements

exhibited that the relative standard deviation was only 4.2%, indicating a good reproducibility. In addition, the specificity was also evaluated by employing five different RNA sequences, including random RNA (0.1 nM), miRNA-122 (0.1 nM), miRNA-141 (0.1 nM), miRNA-199 (0.1 nM), miRNA-210 (0.1 nM), and miRNA-21 (10 pM). As displayed in Fig. 5, the peak current was very high only in the presence of 10 pM miRNA-21, verifying good specificity for miRNA-21 assay.

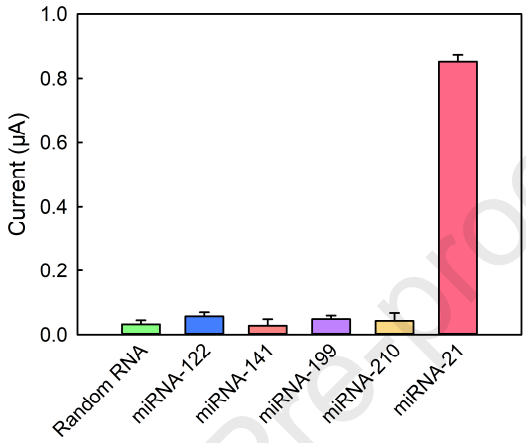

Fig. 5. Specificity of the electrochemical biosensing platform for 10 pM miNRA-21 against 0.1 nM random RNA, miRNA-122, miRNA-141, miRNA-199, and miRNA-210. Error bars are standard deviations of three parallel experiments.

3.6. Recovery test

The recovery tests were executed to evaluate the application potential and analytical reliability of the biosensing platform for the miRNA-21 determination. In short, the real biological sample (human serum) was diluted 10-fold using 10 mM PBS, and then added different concentrations of miRNA-21 (10 fM, 0.1 pM, 10 pM, 100 pM, and 1 nM). As shown in Table 1, the recoveries are 98.2%, 101.0%, 97.3%, 100.9%, and 103.0%, demonstrating that the detection of miRNA-21 in complex biological samples was promising.

Table 1. Recovery test of miRNA-21 detection in 10-fold diluted human serum samples.

Samples (Nos.)	Added	Found	Recovery

1	10 fM	9.82 ± 0.34 fM	98.2%
2	0.1 pM	0.101 ± 0.02 pM	101.0%
3	10 pM	9.73 ± 0.85 pM	97.3%
4	100 pM	100.86 ± 1.57 pM	100.9%
5	1 nM	1.03 ± 0.06 nM	103.0%

4. Conclusions

In summary, an ultrasensitive electrochemical biosensing platform has been successfully built for cascade signal amplification detection of miRNA-21 by combining CRISPR-Cas13a system and CHA reaction. The adoption of CRISPR-Cas13a system can further improve the analytical performance with a detection limit of 2.6 fM, and it also displayed satisfactory specificity and practical utility in complex samples. Moreover, it is easy to detect other miRNAs just through changing the spacer sequence of crRNA, indicating excellent versatility of the proposed biosensing platform. Therefore, this method is expected to be a powerful tool for bioanalysis and clinical molecular diagnostics.

Acknowledgements

This research work was supported by the research foundation of education bureau of Hunan province, China (Grant No. 19C0264 and 19C1705) and the science and technology bureau of Hengyang, China (Grant No. 2019jh010963).

References

[1] E. Wienholds, W.P. Kloosterman, E. Miska, E. Alvarez-Saavedra, E. Berezikov, E.D. Bruijn, H.R. Horvitz, S. Kauppinen, R.H.A. Plasterk, MicroRNA expression in zebrafish embryonic development, Science 309 (2005) 310−311.

[2] C.M. Croce, Causes and consequences of microRNA dysregulation in cancer, Nat. Rev. Genet. 10 (2009) 704−714.

[3] A.E. Pasquinelli, MicroRNAs and their targets: recognition, regulation and an emerging reciprocal relationship, Nat. Rev. Genet. 13 (2012) 271–282.

[4] E. Koscianska, J. Staregaroslan, L.J. Sznajder, M. Olejniczak, P. Galkamarciniak, W.J. Krzyzosiak, Northern blotting analysis of microRNAs, their precursors and RNA interference triggers, BMC Mol. Biol. 2 (2011) 14.

[5] S. Honda, Y. Kirino, Dumbbell-PCR: a method to quantify specific small RNA variants with a single nucleotide resolution at terminal sequences, Nucleic Acids Res. 43 (2015) e77.

[6] N. Rosenfeld, R. Aharonov, E. Meiri, S. Rosenwald, Y. Spector, M. Zepeniuk, H. Benjamin, N. Shabes, S. Tabak, A. Levy, D. Lebanony, Y. Goren, E. Silberschein, N. Targan, A. Benari, S. Gilad, N. Sionvardy, A. Tobar, M. Feinmesser, O. Kharenko, O. Nativ, D. Nass, M. Perelman, A. Yosepovich, B. Shalmon, S. Polak-Charcon, E. Fridman, A. Avniel, I. Bentwich, Z. Bentwich, D. Cohen, A. Chajut, I. Barshack, MicroRNAs accurately identify cancer tissue origin, Nat. Biotechnol. 26 (2008) 462–469.

[7] A.M. Kietrys, W.A. Velema, E.T. Kool, Fingerprints of modified RNA bases from deep sequencing profiles, J. Am. Chem. Soc. 139 (2017) 17074–17081.

[8] Q. Zhou, Y.X. Lin, K.Y. Zhang, M.J. Li, D.P. Tang, Reduced graphene oxide/$BiFeO_3$ nanohybrids-based signal-on photoelectrochemical sensing system for prostate-specific antigen detection coupling with magnetic microfluidic device, Biosens. Bioelectron. 101 (2018) 146–152.

[9] P. Mestdagh, T. Feys, N. Bernard, S. Guenther, C.F. Chen, F. Speleman, J.

Vandesompele, High-throughput stem-loop RT-qPCR miRNA expression profiling using minute amounts of input RNA, Nucleic Acids Res. 36 (2008) e143.

[10] D.W. Kimmel, G. LeBlanc, M.E. Meschievitz, D.E. Cliffel, Electrochemical sensors and biosensors, Anal. Chem. 84 (2012) 685−707.

[11] F. Yang, X.L. Zuo, Z.H. Li, W.P. Deng, J.Y. Shi, G.J. Zhang, Q. Huang, S.P. Song, C.H. Fan, A bubble-mediated intelligent microscale electrochemical device for single-step quantitative bioassays, Adv. Mater. 26 (2014) 4671−4676.

[12] D. Zhu, W. Liu, D.X. Zhao, Q. Hao, J. Li, J.X. Huang, J.Y. Shi, J. Chao, S. Shao, L.H. Wang, Label-free electrochemical sensing platform for microRNA-21 detection using thionine and gold nanoparticles Co-functionalized MoS_2 nanosheet, ACS Appl. Mater. Interfaces 9 (2017) 35597−35603.

[13] C.L. Zhang, D. Li, D.W. Li, K. Wen, X.D. Yang, Y. Zhu, Rolling circle amplification-mediated in situ synthesis of palladium nanoparticles for the ultrasensitive electrochemical detection of microRNA, Analyst 144 (2019) 3817−3825.

[14] R. Hu, G.L. Wang, R. Yuan, R.J. Xu, T.X. Yu, L. Zhong, Q. Zhou, S.J. Ding, An electrochemical biosensor for highly sensitive detection of microRNA-377 based on strand displacement amplification coupled with three-way junction, J. Electroanal. Chem. 789 (2017) 160−166.

[15] Y.Y. Yu, Z.Q. Chen, L.J. Shi, F. Yang, J.B. Pan, B.B. Zhang, D.P. Sun, Ultrasensitive electrochemical detection of microRNA based on an arched probe

mediated isothermal exponential amplification, Anal. Chem. 86 (2014) 8200−8205.

[16] Q.Q. Guo, Y.Q. Yu, H. Zhang, C.X. Cai, Q.M. Shen, Electrochemical sensing of exosomal microRNA based on hybridization chain reaction signal amplification with reduced false-positive signals, Anal. Chem. 92 (2020) 5302−5310.

[17] P. Fu, S. Xing, M.J. Xu, Y. Zhao, C. Zhao, Peptide nucleic acid-based electrochemical biosensor for simultaneous detection of multiple microRNAs from cancer cells with catalytic hairpin assembly amplification, Sens. Actuators B Chem. 305 (2020) 127545.

[18] P. Yin, H.M. Choi, C.R. Calvert, N.A. Pierce, Programming biomolecular self-assembly pathways, Nature 451 (2008) 318–322.

[19] X. Chen, Expanding the rule set of DNA circuitry with associative toehold activation, J. Am. Chem. Soc. 134 (2011) 263–271.

[20] E.H. Xiong, X.X. Yan, X.H. Zhang, Y.M. Li, R.Y. Yang, L.X. Meng, J.H. Chen, A new photoelectrochemical biosensor for ultrasensitive determination of nucleic acids based on a three-stage cascade signal amplification strategy, Analyst 143 (2018) 2799–2806.

[21] M. Jinek, K. Chylinski, I. Fonfara, M. Hauer, J.A. Doudna, E. Charpentier, A programmable dual-RNA-guided DNA endonuclease in adaptive bacterial immunity, Science 337 (2012) 816–821.

[22] P. Horvath, R. Barrangou, CRISPR/Cas, the immune system of bacteria and archaea, Science 327 (2010) 167−170.

[23] J.S. Chen, E. Ma, L.B. Harrington, M.D. Costa, X.R. Tian, J.M. Palefsky, J.A. Doudna, CRISPR-Cas12a target binding unleashes indiscriminate single-stranded DNase activity, Science 360 (2018) 436−439.

[24] S.Y. Li, Q.X. Cheng, J.K. Liu, X.Q. Nie, G.P. Zhao, J. Wang, CRISPR-Cas12a has both *cis*- and *trans*-cleavage activities on single-stranded DNA, Cell Res. 28 (2018) 491−493.

[25] A. East-Seletsky, M.R. O'Connell, S.C. Knight, D. Burstein, J.H. Cate, R. Tjian, J.A. Doudna, Two distinct RNase activities of CRISPR-C2c2 enable guide-RNA processing and RNA detection, Nature 538 (2016) 270−273.

[26] L.B. Harrington, D. Burstein, J.S. Chen, D. Paez-Espino, E. Ma, I.P. Witte, J.C. Cofsky, N.C. Kyrpides, J.F. Banfield, J.A. Doudna, Programmed DNA destruction by miniature CRISPR-Cas14 enzymes, Science 362 (2018) 839−842.

[27] C. Myhrvold, C.A. Freije, J.S. Gootenberg, O.O. Abudayyeh, H.C. Metsky, A.F. Durbin, M.J. Kellner, A.L. Tan, L.M. Paul, L.A. Parham, K.F. Garcia, K.G. Barnes, B. Chak, A. Mondini, M.L. Nogueira, S. Isern, S.F. Michael, I. Lorenzana, N.L. Yozwiak, B.L. MacInnis, I. Bosch, L. Gehrke, F. Zhang, P.C. Sabeti, Field-deployable viral diagnostics using CRISPR-Cas13, Science 360 (2018) 444−448.

[28] C.Q. Yuan, T. Tian, J. Sun, M.L. Wang, E.H. Xiong, M. Cheng, Y.J. Bao, W. Lin, J.M. Jiang, C.W. Yang, Q. Chen, H. Zhang, H. Wang, X.R. Wang, X.B. Deng, X.P. Liao, Y.H. Liu, Z. Wang, G.H. Zhang, X.M. Zhou, Universal and naked-eye gene detection platform based on the clustered regularly interspaced short

palindromic repeats/Cas12a/13a system, Anal. Chem. 92 (2020) 4029−4037.

[29] J.S. Gootenberg, O.O. Abudayyeh, M.J. Kellner, J. Joung, J.J. Collins, F. Zhang, Multiplexed and portable nucleic acid detection platform with Cas13, Cas12a, and Csm6, Science 360 (2018) 439−444.

[30] D.S. Chertow, Next-generation diagnostics with CRISPR, Science 360 (2018) 381−382.

[31] J.S.; Gootenberg, O.O. Abudayyeh, J.W. Lee, P. Essletzbichler, A.J. Dy, J. Joung, V. Verdine, N. Donghia, N.M. Daringer, C.A. Freije, C. Myhrvold, R.P. Bhattacharyya, J. Livny, A. Regev, E.V. Koonin, D.T. Hung, P.C. Sabeti, J.J. Collins, F. Zhang, Nucleic acid detection with CRISPR-Cas13a/C2c2, Science 356 (2017) 438−442.

[32] M.Q. Huang, X.M. Zhou, H.Y. Wang, D. Xing, Clustered regularly interspaced short palindromic repeats/Cas9 triggered isothermal amplification for site-specific nucleic acid detection, Anal. Chem. 90 (2018) 2193−2200.

[33] X.Y. Qiu, L.Y. Zhu, C.S. Zhu, J.X. Ma, T. Hou, X.M. Wu, S.S. Xie, L. Min, D.A. Tan, D.Y. Zhang, L.Y. Zhu, Highly effective and low-cost microRNA detection with CRISPR-Cas9, ACS Synth. Biol. 7 (2018) 807−813.

[34] K.X. Zhang, R.J. Deng, X.C. Teng, Y. Li, Y.P. Sun, X.J. Ren, J.H. Li, Direct visualization of single-nucleotide variation in mtDNA using a CRISPR/Cas9-mediated proximity ligation assay, J. Am. Chem. Soc. 140 (2018) 11293−11301.

[35] K.X. Zhang, R.J. Deng, Y. Li, L. Zhang, J.H. Li, Cas9 cleavage assay for

pre-screening of sgRNAs using nicking triggered isothermal amplification, Chem. Sci. 7 (2016) 4951−4957.

[36] A. East-Seletsky, M.R. O'Connell, D. Burstein, G. J. Knott, J.A. Doudna, RNA targeting by functionally orthogonal type VI-A CRISPR-Cas enzymes, Mol. Cell 66 (2017) 373−383.

[37] K.S. Makarova, F. Zhang, E.V. Koonin, SnapShot: class 2 CRISPR-Cas systems, Cell 168 (2017) 328.

[38] P.W. Qin, M. Park, K.J. Alfson, M. Tamhankar, R. Carrion, J.L. Patterson, A. Griffiths, Q. He, A. Yildiz, R. Mathies, K. Du, Rapid and fully microfluidic Ebola virus detection with CRISPR-Cas13a, ACS Sens. 4 (2019) 1048–1054.

[39] L. Liu, X.Y. Li, J. Ma, Z.Q. Li, L.L. You, J.Y. Wang, M. Wang, X.Z. Zhang, Y.L. Wang, The molecular architecture for RNA-guided RNA cleavage by Cas13a, Cell 170 (2017), 714–726.

[40] Q. Chen, T. Tian, E.H. Xiong, P. Wang, X.M. Zhou, CRISPR/Cas13a signal amplification linked immunosorbent assay for femtomolar protein detection, Anal. Chem. 92 (2020) 573−577

[41] E.H. Xiong, Z.Z. Li, X.H. Zhang, J.W., Zhou, X.X. Yan, Y.Q. Liu, J.H. Chen, Triple-helix molecular switch electrochemical ratiometric biosensor for ultrasensitive detection of nucleic acids, Anal. Chem. 89 (2017) 8830−8835.

[42] A.L. Gui, E. Luais, J.R. Peterson, J.J. Gooding, Zwitterionic phenyl layers: finally, stable, anti-biofouling coatings that do not passivate electrodes, ACS Appl. Mater. Interfaces 5 (2013) 4827–4835.

Highlights

- An ultrasensitive electrochemical biosensing platform based on CRISPR/Cas13a-assisted catalytic hairpin assembly has been developed.
- The developed electrochemical biosensing platform provides a cascade amplified signal for sensitive and accurate detection of miRNA-21.
- The electrochemical biosensing platform shows excellent analytical performance, such as low detection limit, high stability, and specificity.

Declaration of Interest Statement

The authors declare no competing financial interest.